ACS APPLIED MATERIALS & INTERFACES
Research Article
www.acsami.org

Structural Dependences of Localization and Recombination of Photogenerated Carriers in the top GaInP Subcells of GaInP/GaAs Double-Junction Tandem Solar Cells

Zhuo Deng,[†] Jiqiang Ning,[†] Zhicheng Su,[†] Shijie Xu,*[,†] Zheng Xing,[‡] Rongxin Wang,[‡] Shulong Lu,[‡] Jianrong Dong,[‡] Baoshun Zhang,[‡] and Hui Yang[‡]

[†]Department of Physics, HKU-Shenzhen Institute of Research and Innovation (HKU-SIRI), HKU-CAS Joint Laboratory on New Materials, The University of Hong Kong, Pokfulam Road, Hong Kong, China

[‡]Suzhou Institute of Nano-Tech and Nano-Bionics, Chinese Academy of Sciences, Suzhou 215123, China

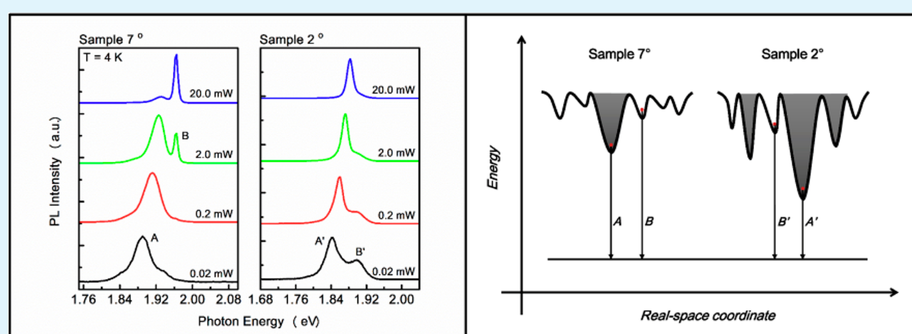

ABSTRACT: In high-efficiency GaInP/GaAs double-junction tandem solar cells, GaInP layers play a central role in determining the performance of the solar cells. Therefore, gaining a deeper understanding of the optoelectronic processes in GaInP layers is crucial for improving the energy conversion efficiency of GaInP-based photovoltaic devices. In this work, we firmly show strong dependences of localization and recombination of photogenerated carriers in the top GaInP subcells in the GaInP/GaAs double-junction tandem solar cells on the substrate misorientation angle with excitation intensity- and temperature-dependent photoluminescence (PL). The entire solar cell structures including GaInP layers were grown with metalorganic chemical vapor deposition on GaAs substrates with misorientation angles of 2° (denoted as Sample 2°) and 7° (Sample 7°) off (100) toward (111)B. The PL spectral features of the two top GaInP subcells, as well as their excitation-power and temperature dependences exhibit remarkable variation on the misorientation angle. In Sample 2°, the dominant localization mechanism and luminescence channels are due to the energy potential minima caused by highly ordered atomic domains; In Sample 7°, the main localization and radiative recombination of photogenerated carriers occur in the atomically disordered regions. Our results reveal a more precise picture on the localization and recombination mechanisms of photogenerated carriers in the top GaInP subcells, which could be the crucial factors in controlling the optoelectronic efficiency of the GaInP-based multijunction photovoltaic devices.

KEYWORDS: *GaInP/GaAs double-junction tandem solar cells, photoluminescence, localization mechanism, radiative recombination*

INTRODUCTION

Ternary alloy GaInP is a technologically important energy material, which is considered to be the most trusted candidate for fabricating top subcell of high-efficiency multijunction tandem solar cells.[1−3] Among the numerous material factors associated with the optimization of the device performance, optical qualities of GaInP layer in the top subcell could be a crucial issue. It has been reported that optical properties of GaInP epilayers could be significantly governed by localized state related processes, because high degree of spontaneous long-range ordering in the group III sublattice atoms in the GaInP microstructure can be obtained by controlling the growth conditions.[4,5] In addition, optical properties of GaInP have been shown to exhibit strong dependence on the growth parameters, such as the growth temperature, substrate misorientation, and growth rate.[6,7] In particular, intensive interests have been focused on the effect of misorientation angle of the lattice-matched GaAs substrate on electronic and optical properties of GaInP. For example, Su et al.[7] found that in the low-temperature PL measurements of several GaInP epilayer samples, the major spectral features, such as peak position, peak number, and full-width at half-maximum (fwhm) displayed remarkable dependence on substrate misorientation. They attributed these dependencies to the different degrees of atomic ordering of group III sublattice caused by the different atomic surface reconstruction rate during the growth.[7] More

Received: October 10, 2014
Accepted: December 5, 2014
Published: December 5, 2014

© 2014 American Chemical Society

recently, He et al.[8] studied optical properties of GaInP epilayers grown on Ge substrate, and they observed that the strong localized state related PL was dominant in the emission when the substrate was misoriented 6° off (001) toward (111). These studies show that carrier localization behaviors and optical properties of GaInP epilayers are strongly dependent on the misorientation angle of the substrate. Therefore, an in-depth investigation of such dependences in GaInP-based multi-junction solar cell structures is particularly appealing, because the electronic structures and optical properties of GaInP epilayer in the top subcell could have a profound impact on the performance of the tandem solar cells.

In this work, we grew two kinds of GaInP/GaAs double-junction tandem solar cells on GaAs substrates with misorientation angles of 2° and 7° off (100) toward (111)B, respectively, with metalorganic chemical vapor deposition (MOCVD), and then conducted a detailed investigation on the localization and luminescence mechanism of photo-generated carriers in the top GaInP subcells of the two structures with the excitation-intensity- and temperature-dependent PL techniques. Indeed, the two kinds of samples show very dissimilar luminescence behaviors. On the basis of the experimental results and analysis, we attribute the large difference in luminescence behavior between the two kinds of samples to the pronounced variation in microstructure (i.e., the degree of spontaneous atomic ordering) between the GaInP layers grown on substrates with different misorientation angles. The very different spontaneous ordering degrees of Ga and In atoms in the alloys cause the distinctive localization mechanisms and luminescence behaviors of photogenerated carriers in the top GaInP subcells.

■ EXPERIMENTAL DETAILS

The two kinds of GaInP/GaAs double-junction tandem solar cell structures studied in this work were grown on stepped p^+-GaAs substrates with different misorientations with MOCVD. The misorientation angles of the two stepped (100) substrate surfaces were 2° and 7° off (100) toward (111)B. The structure and growth details of the two devices have been described elsewhere previously.[9,10] The structure design and the growth conditions of the two samples were nominally identical. The only structural variation between them was the misorientation angle of the p^+-GaAs substrate. For convenience, they were referred to as Sample 2° and Sample 7°, respectively.

In the PL measurements, the excitation source was the 514.5 nm line emitted from a Coherent Ar−Kr ion mixed gas laser. The solar cell samples were mounted on the coldfinger of Janis SHI-4−5 closed-cycle cryostat with a varying temperature range from 4 to 300 K. The excitation power was modulated from 0.02 to 20 mW by intercepting the excitation optical path with neutral density filters. The luminescence signal was collected by the lens pairs and dispersed by a Jobin Yvon SPEX750M monochromator, which was later detected by a Hamamatsu R928 photomultiplier tube. The electrical signal from the detector was amplified by a Stanford Research SR830 lock-in amplifier in conjunction with a chopper so as to magnify the signal-to-noise-ratio.

■ RESULTS AND DISCUSSION

The excitation intensity-dependent PL spectra recorded from the two top GaInP subcells at 4 K are shown in Figure 1, and the corresponding evolution of the PL peak energy and integrated intensity of the main spectral features on excitation level were extracted from Figure 1 and depicted in Figures 2 and 3, respectively. As shown in Figure 1, at the lowest excitation power of 0.02 mW, the emission band from Sample 7° consists of a single main structure located at 1.890 eV (labeled as "A"). As the excitation level increases the peak

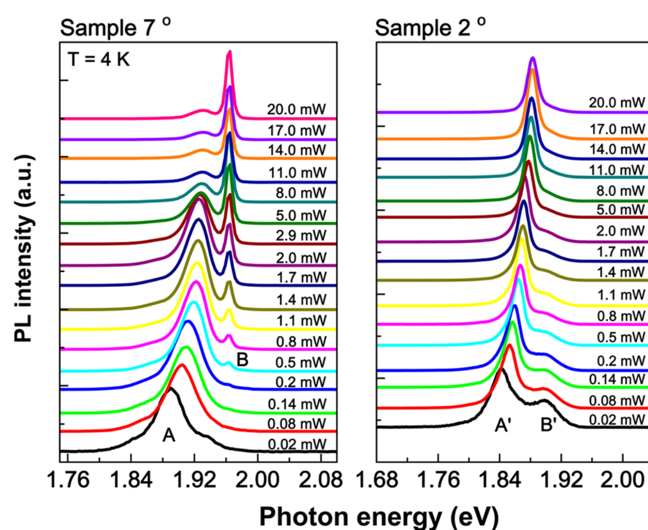

Figure 1. Excitation power-dependent PL spectra recorded from the two top GaInP subcells at 4 K. The emission peaks are labeled with different letters accordingly.

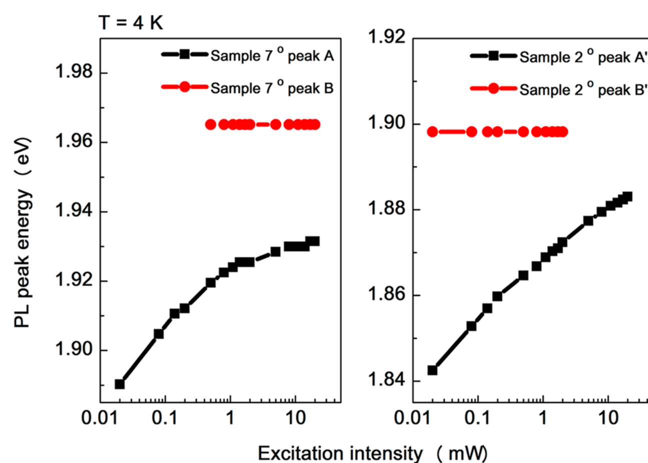

Figure 2. Energies of the PL peaks of the two samples at 4 K versus the excitation power (semilogarithmic scale).

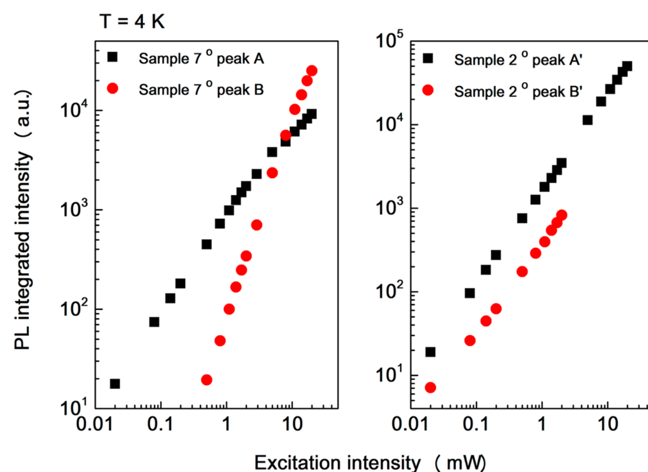

Figure 3. Integrated intensities of the PL emission peaks of the two samples at 4 K versus the excitation power (full logarithmic scales).

position of structure A demonstrates a very clear blue-shift, and a new structure (labeled as "B") located at 1.965 eV becomes observable from 0.5 mW. Compared with structure A, structure B has a much narrower full-width at half-maximum (fwhm) of 10.3 meV. In the analysis of PL emission of the typical p−n junction-based tandem solar cell structure, for the configuration of n $^+$-on-p shallow homojunction subcell, it is assumed that the PL transition from the much narrower and heavily doped n-type emitter is too weak to be detected, and the emission from the thin depletion region can be negligible.[11] Therefore, in a good enough approximation, the light emissions from the top GaInP subcells in our samples are considered to be mainly from the p-type base layer.[9] From Figure 2, it is clear that the energetic position of peak B is almost independent with the excitation intensity. In addition, from Figure 3, the integrated intensity of peak B increases much faster than that of peak A. In particular, an obvious PL dominancy switching from peak A to peak B occurs at the excitation level of ∼5 mW. When the excitation intensity further increases to 20 mW, the PL spectrum measured from the subcell is completely dominated by peak B, and peak A becomes a weak shoulder with a total shift amount of ∼41 meV. Similar remarkable "crossing over" in PL intensity between the two emission peaks with varying excitation intensity was observed in the GaInP epilayers by DeLong et al.[5] Comparatively, the excitation-intensity dependence of PL emission in Sample 2° shows a significant difference with that observed in Sample 7°. As can be seen from Figure 1, the PL spectrum at the lowest excitation level displays two emission bands, with the stronger peak located at 1.842 eV (labeled as " A′ ") and the weaker peak at 1.898 eV (labeled as " B′ "). As the excitation level increases, the energy of peak A′ also shows remarkable blue-shift, whereas the energy of peak B′ shows negligible shift, similar to the results observed in Sample 7° as shown in Figure 2. On the other hand, as seen from Figure 3, the PL intensity of peak A′ increases rapidly with increasing excitation level, whereas the PL emission of peak B′ becomes indistinguishable at the excitation intensity ∼5 mW. When the excitation power reaches 20 mW, the PL spectrum is dominant by peak A′, and its peak energy shifts to 1.883 eV, which shows a total shift amount of ∼41 meV commensurable with that in Sample 7°. It is notable that the energetic positions of the main PL emissions in Sample 2° are remarkably lower than those in Sample 7°. The excitation-intensity dependences observed in both the subcells suggest that carrier localization may play a very important role in determining the radiative process of carriers in the GaInP subcells, and the localization behaviors of photogenerated carriers are strongly governed by the variations of microstructures in GaInP, which are altered by the misorientation angle of the GaAs substrate.[5,6]

To further unveil the nature of carrier localization and light emission, we measured PL spectra as a function of temperature on the two GaInP subcells. The results are plotted in Figure 4. Throughout the measurements, the excitation intensity was kept constant at 20 mW, such that the PL spectral conditions recorded at 4 K are identical to those obtained at the highest excitation level (20 mW) depicted in Figure 1. In Sample 7°, the emission spectrum at 4 K is predominated by peak B located at 1.965 eV, whereas the much weaker shoulder at peak A is observed at 1.931 eV. As the temperature increases, the emission at peak B demonstrates a clear red-shift toward the lower energy direction, as shown on the left figure in Figure 5, and the spectral line shape becomes broader and more asymmetric. On the other hand, the PL intensity of peak A

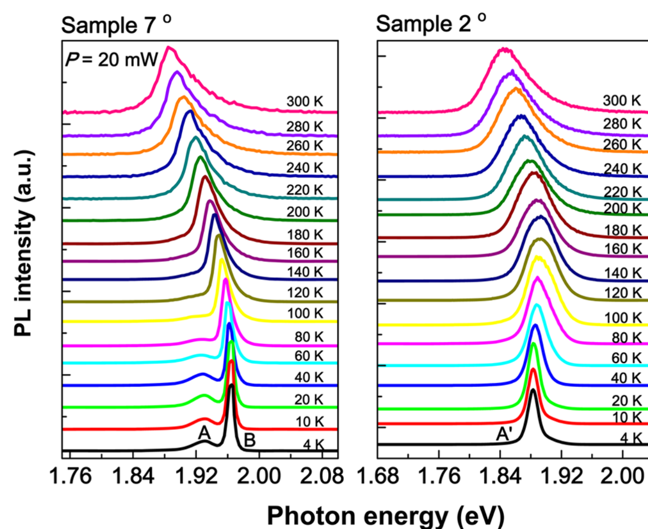

Figure 4. PL spectra recorded from the two top GaInP subcells as a function of temperature at the excitation power of 20 mW. The letters labeled on the emission peaks are in line with those in Figure 1.

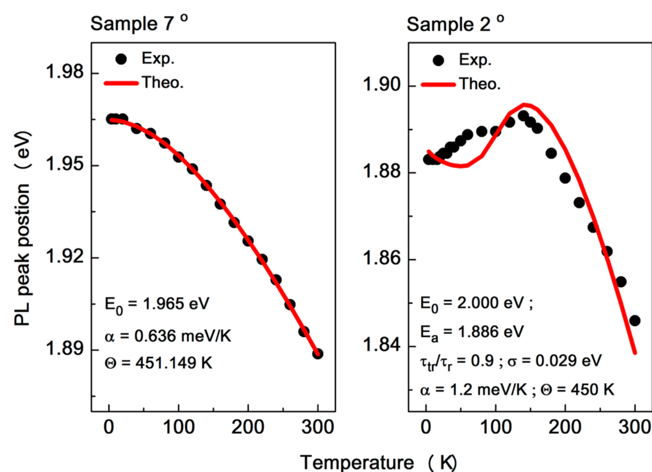

Figure 5. Temperature evolutions of the emission energy of peak B (left) and peak A′ (right) excerpted from the PL spectra of Sample 7° and Sample 2° depicted in Figure 4, respectively. The solid curve in the left figure is the fitting with the Varshni's empirical formula, whereas the solid curve in the right figure results from fitting with eqs 2 and 3, and the relevant parameters adopted in the fittings are also labeled, respectively.

quickly diminishes, and becomes unobservable at the temperature ∼120 K. At 300 K, the PL spectrum is solely determined by peak B with the emission energy shifted to 1.889 eV. The line shape transforms completely to the asymmetric nature with a longer tail attached at the higher energy side, similar to the emission line shape observed in room temperature electroluminescence (EL) measurements on the same subcell structure.[9] The peak position shift of peak B in Sample 7° with temperature follows the band gap shrinking pattern predicted by the well-known Varshni's empirical formula.

In sharp contrast to the case in Sample 7°, the PL spectra of Sample 2° are dominated by peak A′, as shown in Figure 4. The temperature dependence of peak position of peak A′ deviates extraordinarily from the band gap shrinking curve predicted by the Varshni's empirical formula. At the temperature of 4 K, the energy of peak A′ locates at 1.883 eV. When temperature increase, however, the emission peak energy shifts to the higher

energy side first, and this blue-shift continues until the temperature reaches ∼140 K, where the emission energy has reached 1.893 eV. When the temperature rises to >140 K, the temperature evolution of the emission peak returns to display the red-shift behavior as described by the material band gap temperature shrinkage. At 300 K, the peak A′ is located at the energetic position of 1.846 eV. The evolution tendency of emission energy of peak A′ with temperature is depicted in the right figure of Figure 5. As can be seen, an abnormal dependence of the emission peak position on temperature is clearly demonstrated, with the critical point located at ∼140 K. Such anomalous temperature dependence has been observed in the GaInP epilayers which possess partial degree of group III atomic spontaneous ordering in the sublattice.[4,8,12,13] In conjunction with the observed much lower emission energy and the excitation intensity-induced blue-shift of peak position, the anomalous temperature dependence of the PL peak indicates that the emission at peak A′ in Sample 2° shall result from the radiative recombination of carriers localized at the quantum confinement states by local atomic ordering. Such local atomic ordering domains embedded within disordered matrix with larger potential energy can introduce localized states with lower energies.[13] When carriers bounded at these localized states recombine radiatively, polarized light emission with lower peak energy may be observed in GaInP alloy.[13] It has been pointed out by Li et al. that thermally induced redistribution of carriers within localized states can result in anomalous temperature dependence of PL peak.[14] They also developed a generalized localized-state-ensemble (LSE) luminescence model and successfully interpreted anomalous luminescence behaviors observed in a variety of materials.[15,16]

According to the LSE model, luminescence spectrum from a localized-state-ensemble with a Gaussian type density of states can be described by[15]

$$I_{\mathrm{PL}} \propto \rho(E)f(E, T) = \rho_0 e^{-(E-E_0)^2/2\sigma^2}\frac{1}{e^{(E-E_a)/k_BT+\tau_{tr}/\tau_r}} \quad (1)$$

where E is the emission photon energy, $\rho(E) = \rho_0 e^{-(E-E_0)^2/2\sigma^2}$; represents a Gaussian type distribution of localized states in the material with its center at E_0 and width of σ; E_a is the thermal activation energy that depends on material, k_BT is the Boltzmann thermal energy, and τ_{tr} and τ_r are the time constants of localized carriers for thermal activation and radiative luminescence, respectively. From eq 1 and taking into account the band gap shrinkage described by the Varshni's empirical formula, the temperature dependence of localized carrier PL peak energy can be derived as[14,15]

$$E(T) = \left(E_0 - \frac{\alpha T^2}{T + \Theta}\right) - xk_BT \quad (2)$$

where the bracketed term is the Varshni's empirical formula in which the Varshni parameter and Debye temperature of material are represented by α and Θ, respectively. The second term is arisen from the thermal redistribution of localized carriers, and the parameter x is found by numerically solving the following nonlinear equation[14,15]

$$xe^x = \left[\left(\frac{\sigma}{k_BT}\right)^2 - x\right]\left(\frac{\tau_r}{\tau_{tr}}\right)e^{(E_0-E_a)/k_BT} \quad (3)$$

The observed anomalous temperature dependence of the energetic position of peak A′ can be fitted by eqs 2 and 3, and the fitting result is shown by the solid curve in Figure 5. The parameters adopted in the fitting are also labeled. The clear blue-shift of the emission energy below ∼140 K could be interpreted as one consequence of carriers' thermal redistribution within the localized states, as the carriers could gain thermal energy when temperature increases and transfer from localized states at lower energy to localized states at higher energy.[14] A similar mechanism was also employed to interpret the temperature induced blue-shift observed in the antistokes PL emission in the partially ordered GaInP/GaAs interface system.[17] The thermal transfer and redistribution of carrier may be also responsible for the transformation of the PL spectral line shape of peak A′ into the asymmetric characteristic, as displayed in Figure 4. In contrast to the case of Sample 2°, the dominant radiative recombination of photogenerated carriers in Sample 7° occurs in its major disordered regions. Therefore, the temperature dependence of peak position of peak B follows the prediction by the Varshni's empirical formula.

At last, we attempt to establish a consistent picture to explain the significant distinction observed in the PL properties of the two kinds of GaInP subcells. It is known that the CuPt-B type spontaneous ordering in group III sublattice atoms may occur naturally in many ternary and quaternary alloys, including the GaInP epitaxially grown on the lattice-matched GaAs substrate. The group III Ga and In atoms occupy the alternate lattice planes along the two possible (111)B directions by forming the superlattice-like layered structure, and this long-range ordering has been demonstrated to significantly alter the electronic and optical properties of the GaInP structure, such as emission band gap narrowing and optical anisotropy.[6,13] The degree of atomic ordering, which is characterized by (1) the atomic fraction of Ga and In atoms on one (111)B lattice plane within the ordered domain; (2) the size; and (3) the density of ordered domain, can be quantitatively described by the long-range ordering parameter, η, whose value can be estimated through the low-temperature PL measurement according to the following formula[18]

$$\eta = \sqrt{\frac{2.005 - E_g(\eta)}{0.471}} \quad (4)$$

where $E_g(\eta)$ represents the band gap of ordered GaInP characterized by η and can be found by the PL peak energy at low temperature regime (<10 K), and 2.005 eV represents the band gap value of the nominally fully disordered GaInP epilayer at the same temperature. The degree of ordering in GaInP can be sensitively modified by the growth conditions.[5] One of such growth parameter correlation on the degree of ordering which has been studied extensively is the misorientation angle of the GaAs substrate. Previous studies show that at certain growth temperatures and growth rates, the CuPt-B type ordered structures of GaInP alloy can be intentionally controlled by the substrate misorientation, as evidenced by transmission electron diffraction and PL measurements.[7,8] In the alloy grown with larger substrate misorientation, the degree of ordering would be lower, leading to a relatively larger band gap. In the alloy grown with smaller misoriented angle, the reconstruction process facilitates a higher degree of ordering, resulting in a lower band gap. Meanwhile, the atomic ordering domains with higher degree can cause deeper potential wells which could provide stronger confinement (localization) to carriers. Therefore,

different localized state distributions between the two kinds of GaInP alloys could bring out dissimilar PL behaviors as observed in the present study.

To graph the idea, a schematic representation showing the potential energy profiles of the two kinds of GaInP alloys with different degrees of local atomic ordering is depicted in Figure 6. The ordered domains are indicated by the shaded regions,

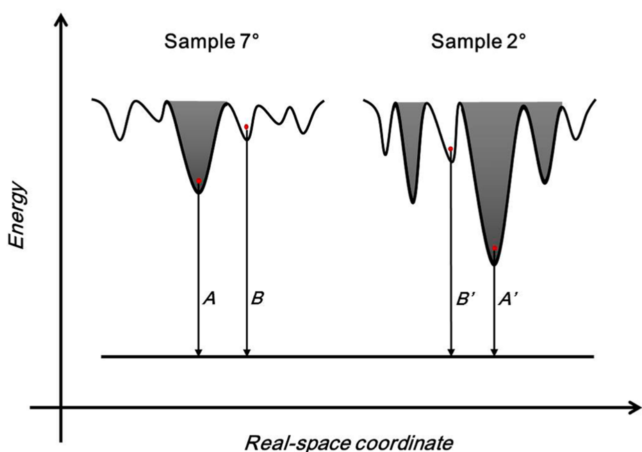

Figure 6. Schematic representations of the potential energy profile of localized states within the two top GaInP subcells. The shaded potential wells depict the ordered domains, while the unshaded potential minima represent the randomly disordered matrices. The PL emission processes corresponding to the emission peaks labeled in Figures 1 and 4 are indicated by the vertical arrows with letters.

while the unshaded areas represent the disordered matrices. On the basis of the PL experimental results and the GaInP atomic microstructures argued above, the degree of ordering of Sample 7° is considered to be lower. The long-range ordering parameter η of Sample 7° can be estimated by eq 4, by taking $E_g(\eta)$ with a value of 1.965 eV as measured for peak B at the temperature of 4 K

$$\eta = \sqrt{\frac{2.005 - 1.965}{0.471}} \approx 0.085. \tag{5}$$

The potential profile comprises a broad distribution of fluctuating potential minima with a low density of small size ordered domains embedded into it. In this case, in the excitation intensity-dependent PL measurement, we shall observe peak A, the radiative recombination of carriers localized in the ordered domain at low excitation level first. With increasing the excitation level the band filling effect in these localized states takes place, in which the photogenerated carriers may occupy the localized states at higher energy, leading to the blue-shift of PL emission energy.[5] When the excitation level further increases, the PL emission dominancy is switched from peak A to peak B due to the low density of ordered domains. Peak B is from the radiative recombination of carriers localized at shallow but high density of energy states because of the randomly disordered matrix.

Comparatively, the degree of ordering of Sample 2° is considered to be higher. Similarly, the long-range ordering parameter η of Sample 2° can be estimated by eq 4 by taking $E_g(\eta)$ with a value of 1.883 eV as measured for peak A′ at the temperature of 4 K

$$\eta = \sqrt{\frac{2.005 - 1.883}{0.471}} \approx 0.259. \tag{6}$$

Apparently the ordering parameter of Sample 2° is much higher than that of Sample 7°. In this circumstance, the energy potential profile consists of a higher density of large size ordered domains embedded in the disordered matrices. One important supporting point of this attribution is the much lower PL emission energy (i.e., 1.846 eV at 300 K) compared with that of Sample 7°. The localization depth of carriers in the ordered domains is averagely much deeper, as schematically shown on the right in Figure 6. In the excitation intensity-dependent PL measurement, at low excitation levels the PL emission spectra of Sample 2° are dominated by the emission at peak A′. As the light excitation level becomes higher, the peak energy blue-shift induced by the band filling is also remarkable for peak A′. However, unlike the case of Sample 7°, high density of ordered domains in Sample 2° ensure the dominance of peak A′ in the excitation intensity-dependent PL spectra in the interested excitation intensity range. Temperature dependence of peak A′ also shows anomalous behavior due to the thermal redistribution of carriers within the localized states caused by high density of ordered domains, as we have already discussed above.

■ CONCLUSION

In conclusion, significant dependences of carrier localization and luminescence behaviors on the substrate misorientation angle in the top GaInP subcells of two kinds of GaInP/GaAs double-junction tandem solar cell structures were revealed by steady-state PL spectroscopy. Very different potential energy profiles caused by different microstructure configurations were proposed to interpret the observed dissimilar PL behaviors of the two samples. Our results show that the localization environment and radiative recombination of photogenerated carriers in the top GaInP subcells can be largely modulated by changing the substrate misorientation angle, which could be an important factor being worth of particular attention for optimizing the performance of high-efficiency GaInP-based multijunction solar cells.

■ AUTHOR INFORMATION

Corresponding Author

* Tel.: +852 2241 5636. Fax: +852 2559 9152. E-mail: sjxu@hku.hk.

Notes

The authors declare no competing financial interest.

■ ACKNOWLEDGMENTS

This work was financially supported by NSFC Grants (Grant 11374247).

■ REFERENCES

(1) Olson, J. M.; Kurtz, S. R.; Kibbler, A. E.; Faine, P. A 27.3% Efficient $Ga_{0.5}In_{0.5}P$/GaAs Tandem Solar Cell. *Appl. Phys. Lett.* **1990**, *56*, 623−625.

(2) Takamoto, T.; Ikeda, E.; Kurita, H.; Ohmori, M.; Yamaguchi, M.; Yang, M. J. Two-Terminal Monolithic $In0_{.5}Ga_{0.5}P$/GaAs Tandem Solar Cells with a High Conversion Efficiency of Over 30%. *Jpn. J. Appl. Phys.* **1997**, *36*, 6215−6220.

(3) NREL Solar Cell Record: Conversion-efficiency Record for a Two-junction Solar Cell Measured Under One-sun Illumination. www.

sciencedaily.com/releases/2013/06/130625141210.htm (accessed January 27).
(4) DeLong, M. C.; Mowbray, D. J.; Hogg, R. A.; Skolnick, M. S.; Hopkinson, M.; David, J. P. R.; Taylor, P. C.; Kurtz, S. R.; Olson, J. M. Photoluminescence, Photoluminescence Excitation, and Resonant Raman Spectroscopy of Disordered and Ordered $Ga_{0.52}In_{0.48}P$. *J. Appl. Phys.* **1993**, *73*, 5163−5172.
(5) DeLong, M. C.; Taylor, P. C.; Olson, J. M. Excitation Intensity Dependence of Photoluminescence in $Ga_{0.52}In_{0.48}P$. *Appl. Phys. Lett.* **1990**, *57*, 620−622.
(6) Su, L. C.; Ho, I. H.; Stringfellow, G. B. Ordering in GaInP Grown at Low Temperatures. *J. Cryst. Growth* **1995**, *146*, 558−563.
(7) Su, L. C.; Ho, I. H.; Stringfellow, G. B. Effects of Substrate Misorientation and Growth Rate on Ordering in GaInP. *J. Appl. Phys.* **1994**, *75*, 5135−5141.
(8) He, W.; Lu, S. L.; Dong, J. R.; Zhao, Y. M.; Ren, X. Y.; Xiong, K. L.; Li, B.; Yang, H.; Zhu, H. M.; Chen, X. Y.; Kong, X. Structural and Optical Properties of GaInP Grown on Germanium by Metal-organic Chemical Vapor Deposition. *Appl. Phys. Lett.* **2010**, *97*, 121909.
(9) Deng, Z.; Wang, R. X.; Ning, J. Q.; Zheng, C. C.; Bao, W.; Xu, S. J.; Zhang, X. D.; Lu, S. L.; Dong, J. R.; Zhang, B. S.; Yang, H. Radiative Recombination of Carriers in the $Ga_xIn_{1-x}P$/GaAs Double-junction Tandem Solar Cells. *Sol. Energy Mater. Sol. Cells* **2013**, *111*, 102−106.
(10) Deng, Z.; Wang, R. X.; Ning, J. Q.; Zheng, C. C.; Xu, S. J.; Xing, Z.; Lu, S. L.; Dong, J. R.; Zhang, B. S.; Yang, H. Super Transverse Diffusion of Minority Carriers in $Ga_xIn_{1-x}P$/GaAs Double-junction Tandem Solar Cells. *Sol. Energy* **2014**, *110*, 214−220.
(11) Yang, M. J.; Yamaguchi, M.; Takamoto, T.; Ikeda, E.; Kurita, H.; Ohmori, M. Photoluminescence Analysis of InGaP Top Cells for High-efficiency Multi-junction Solar Cells. *Sol. Energy Mater. Sol. Cells* **1997**, *45*, 331−339.
(12) Kondow, M.; Minagawa, S.; Inoue, Y.; Nishino, T.; Hamakawa, Y. Anomalous Temperature Dependence of the Ordered $Ga_{0.5}In_{0.5}P$ Photoluminescence Spectrum. *Appl. Phys. Lett.* **1989**, *54*, 1760−1762.
(13) Ning, J. Q.; Xu, S. J.; Deng, Z.; Su, Z. C. Polarized and Non-polarized Photoluminescence of $GaInP_2$ Alloy with Partial CuPt-type Atomic Ordering: Ordered Domains vs. Disordered Regions. *J. Mater. Chem. C* **2014**, *2*, 6119−6124.
(14) Li, Q.; Xu, S. J.; Cheng, W. C.; Xie, M. H.; Tong, S. Y.; Che, C. M.; Yang, H. Thermal Redistribution of Localized Excitons and Its Effect on the Luminescence Band in InGaN Ternary Alloys. *Appl. Phys. Lett.* **2001**, *79*, 1810−1812.
(15) Li, Q.; Xu, S. J.; Xie, M. H.; Tong, S. Y. A Model for Steady-state Luminescence of Localized-state Ensemble. *Europhys. Lett.* **2005**, *71*, 994−1000.
(16) Li, Q.; Xu, S. J.; Xie, M. H.; Tong, S. Y. Origin of the 'S-shaped' Temperature Dependence of Luminescent Peaks from Semiconductors. *J. Phys.: Condens. Matter* **2005**, *17*, 4853−4858.
(17) Xu, S. J.; Li, Q.; Dong, J. R.; Chua, S. J. Interpretation of Anomalous Temperature Dependence of Anti-Stokes Photoluminescence at $GaInP_2$/GaAs Interface. *Appl. Phys. Lett.* **2004**, *84*, 2280−2282.
(18) Song, J. D.; Kim, J. M.; Lee, Y. T. Growth of highly disordered InGaP on (100) GaAs by molecular beam epitaxy with a GaP decomposition source. *Appl. Phys. A: Mater. Sci. Process.* **2001**, *72*, 625−627.